ON THE RESONANCES OF SURFACE BREAKING CRACKS

S. Ayter and B. A. Auld
Edward L. Ginzton Laboratory
Stanford University, Stanford, California 94305

ABSTRACT

The resonance phenomenon observed in Rayleigh wave scattering from surface-breaking cracks has been investigated using Freund's results on reflection of Rayleigh waves from an infinite crack edge. To model the crack as a section of acoustic waveguide, resonances are treated as standing waves in the length and depth directions. The model takes both faces of the crack into consideration, and this makes it possible to explain the observations of all order resonances in the length direction for excitation by a Rayleigh wave beam at normal incidence. Calculations are made for rectangular and half-penny shaped cracks and differences between the two cases are discussed.

INTRODUCTION

One of the sources of data for the estimation of dimensions of surface breaking cracks is their frequency response. Experimental results have shown that crack response shows resonance-like variations in the short wavelength regime.[1,2] Some of those variations were found to be associated with the length and depth of the cracks,[2] however previous interpretations fail to explain the observation of all order length resonances for a symmetric excitation in length dimension. Such interpretations take only the illuminated face of the crack into account, neglecting the effect of its back face.[1,2,3] Freund has demonstrated in Reference 4 that the crack edge couples the fields between the front and back faces and the coupling parameters have been calculated. Using those parameters, he also showed that an infinite slit structure can guide waves if the edge separation is wide enough and he derived dispersion relations for the modes of this structure.[5] In this study, these calculations are reviewed and a model is proposed for surface crack resonances, using the waveguide modes obtained from the calculations.

RAYLEIGH WAVE PROPAGATION IN TWO DIMENSIONS

A surface wave, traveling on the plane defined by x and y axes and decaying in z direction can be expressed in terms of its component along the decay direction (z-axis) only.[6] The particle velocity component along the decay direction then can be written as

$$V_z(x,y,z) = f(z)\,\bar{V}_z(x,y)e^{i\omega t} \qquad (1)$$

where $\bar{V}_z(x,y)$ satisfies the two-dimensional reduced wave equation

$$\left[\nabla^2 + (\omega/V_R)^2\right]\bar{V}_z(x,y) = 0 \qquad (2)$$

and $f(z)$ is a known function describing the decay along the depth of the plate. The other components of particle velocity can easily be found once $V_z(x,y)$ is known.[6]

REFLECTION OF RAYLEIGH WAVES FROM AN INFINITE CRACK EDGE

Consider a semi-infinite crack with its edge along the y axis and faces in the x-y plane for $x > 0$. The faces are assumed to lie on either side of the $z = 0$ plane. They are denoted as the z^+ and z^- faces. Let a Rayleigh wave on the z^+ face be incident obliquely on the edge, its propagation vector lying at an angle θ with the crack edge (y-axis). The incident wave will yield two scattered surface waves, one on each face of the crack. Bulk waves will also be radiated into the medium outside the crack when the angle of incidence θ is large enough. Of the two scattered surface waves, the one on z^+ face will be called the reflected wave (with reflection coefficient $R(\theta)$) and the one on z^- face will be identified as the transmitted wave (with transmission coefficient $T(\theta)$). The reflection and transmission coefficients are defined in terms of the component of particle displacement in the z direction.

Using the three-dimensional representation theorem due to deHoop, Freund solved this scattering problem and calculated the parameters $R(\theta)$ and $T(\theta)$.[4] When the angle of incidence $\theta < \theta_{CR,S} = \cos^{-1}(V_R/V_S)$, ($V_R$ - Rayleigh wave velocity; V_S - shear wave velocity), the incident wave cannot excite propagating bulk waves and all the power is scattered into surface waves on the z^+ and z^- faces. That is

$$|R(\theta)|^2 + |T(\theta)|^2 = 1 \quad \text{for} \quad \theta < \theta_{CR,S} \qquad (3)$$

In the same angular region, the phases of the reflection and transmission coefficients satisfy the following relation,

$$\Delta(\theta) = \arg T(\theta) - \arg R(\theta) = \frac{\pi}{2} \quad \text{for} \quad \theta < \theta_{CR,S} \qquad (4)$$

For $\theta > \theta_{CR,S}$ the incident wave is able to excite radiating shear waves which can carry energy away from the crack edge; and, for $\theta > \theta_{CR,L} = \cos^{-1}(V_R/V_L)$, ($V_L$ - longitudinal wave velocity) $R(\theta)$ and $T(\theta)$ approach small purely imaginary quantities with magnitudes in the order of 0.1. Under this condition $|T(\theta)| > |R(\theta)|$.

Crack Modeling. We first solve the guidance problem for the infinite crack geometry, using the transverse resonance technique, then impose the finite length of the crack in order to find its resonances. For the partial waves to be used in transverse resonance analysis, we will use solutions of Eq. (2) in an appropriate coordinate system.

(a) Rectangular crack: Rectangular crack geometry is shown in Fig. 1(a). The solutions of Eq. (2) are ordinary plane waves propagating in x-y plane. Since the power is confined to surface waves only for $\theta < \theta_{CR,S}$, only the partial waves with incidence angle satisfying that relation will be considered. Otherwise the waveguide modes will be very lossy and will not produce good resonances.

Slit waveguide modes. The slit waveguide geometry is shown in Fig. 1(b). On each face of the crack we assume two partial waves propagating in opposite x directions with the same angle of incidence at $x = \pm L/2$, L being the width of the slit. We will assume that each partial wave reflects from an edge as if the other edge were absent. The validity of this assumption depends on the relative magnitude of the slit width L with respect to the Rayleigh wavelength λ_R, and for the frequency range of interest to us, where $2\pi(L/\lambda_R) > 1$, this assumption is verified by Freund.[5] Considering the configuration in Fig. 1(b), the partial waves $P_i, i=1,2,3,4$ can be expressed as follows:

$$\begin{aligned}
&P_1: A_1 \exp(-ik_x x - \beta_G y) \quad \text{with decay in +z direction}\\
&P_2: A_2 \exp(-ik_x x - \beta_G y) \quad \text{with decay in -z direction}\\
&P_3: A_3 \exp(ik_x x - \beta_G y) \quad \text{with decay in +z direction}\\
&P_4: A_4 \exp(ik_x x - \beta_G y) \quad \text{with decay in -z direction}
\end{aligned} \tag{5}$$

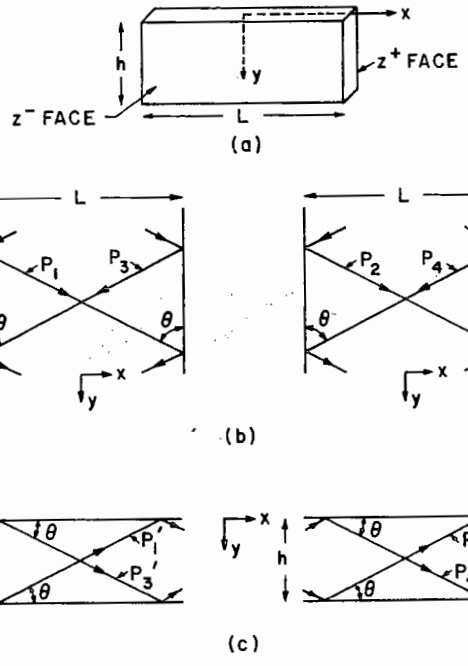

FIG. 1. (a) Rectangular crack geomery;
(b) Partial waves for slit waveguide;
(c) Partial waves for crack waveguide.

Writing the boundary conditions at $x = \pm L/2$ and keeping in mind that R and T are defined in terms of $+z$ components of the partial waves, one obtains the following eigenvalue expression:

$$e^{ik_x L}\begin{pmatrix} A_1\\ A_2\\ A_3\\ A_4\end{pmatrix} = \begin{pmatrix} 0 & 0 & R & -T\\ 0 & 0 & -T & R\\ R & -T & 0 & 0\\ -T & R & 0 & 0\end{pmatrix}\begin{pmatrix} A_1\\ A_2\\ A_3\\ A_4\end{pmatrix} \tag{6}$$

Each solution of Eq. (6) defines a modal field distribution. The solutions are tabulated in Table 1. Mode identifications are made considering Fig. 1(b), where E and O stands for even (symmetric) and odd (antisymmetric) variations along the direction defined by the subscripts x and z. The modes are consistent with the symmetry of the structure.

Table 1. Slit waveguide modes

A_1	A_2	A_3	A_4	$e^{ik_x L}$	Mode Identification
1	1	1	1	R - T	$E_x E_z$
1	-1	1	-1	R + T	$E_x O_z$
1	1	-1	-1	-(R - T)	$O_x E_z$
1	-1	-1	1	-(R + T)	$O_x O_z$

Dispersion relations can be obtained in the following manner. From the fifth column, one can write

$$k_x L = \arg(R \pm T) + 2m\pi \tag{7a}$$

and plot the RHS as a function of θ. Considering Fig. (1b), the following relation can readily be shown to be required

$$k_x L = \beta_G L \tan\theta \tag{7b}$$

Taking $\beta_G L$ as a parameter, $k_x L$ vs θ can also be plotted. Intersection of two curves for $\theta < \theta_{CR,S}$ determines k_x (and β_G) for the propagating modes. This is illustrated in Fig. 2 where dashed lines correspond to Eq. (7b) and solid lines correspond to Eq. (7a). This figure is for a Poisson ratio of 0.25, for which $\theta_{CR,S} = 23.2°$. The following points are worth considering:

1) For the lowest order propagating mode, $\beta_G L \cong 2$, $k_x L \sim \pi/4$, $k_R L \sim 2.2$. Therefore the analysis is valid only for cracks with $L > 0.4\,\lambda_R$.

2) Since $\theta < \theta_{CR,S} = 23.2°$, the guided wave velocity $V_G = V_R/\cos\theta$ is very near to the Rayleigh wave velocity.

Crack waveguide modes. Consider the crack waveguide shown in Fig. 1(c). Through a similar analysis, one can analyze the waveguide modes supported by this structure, if scattering coefficient of Rayleigh wave at the upper edge of a crack face is known. To our knowledge this problem has not been solved for other than normal incidence.[7] We will denote the relevant reflection coefficient by $\bar{R}(\theta)$ and either approximate it or treat it as an adjustable parameter to be fitted to experimental results. Scattering at the bottom of the crack is treated as in the previous subsections, by the Freund theory. Although the crack waveguide has no symmetry in the plane of the crack, it is symmetrical with respect to the z direction. The analysis shows that

modes of even and odd symmetry with respect to the z direction have the properties listed in Table 2.

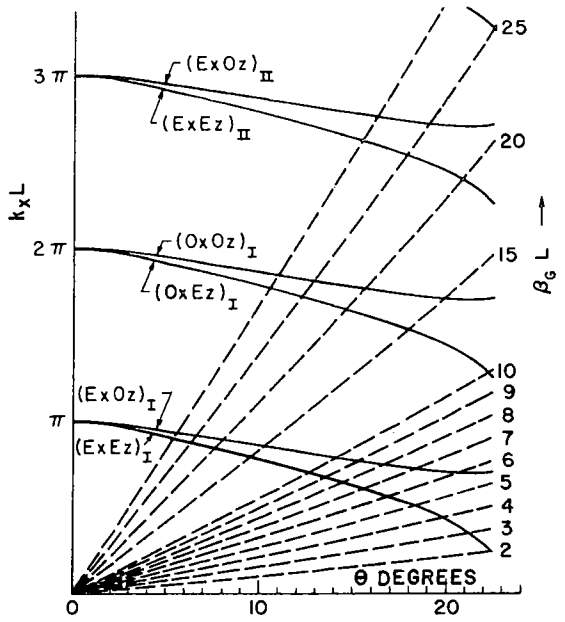

FIG. 2. Graphical solution of dispersion equation for slit waveguide modes.

Table 2. Crack waveguide modes

A_1	A_2	A_3	A_4	$e^{i2k_y h}$	Mode Identification
1	1	$\bar{R}$	$\bar{R}$	$\bar{R}(R-T)$	E_z
1	-1	$\bar{R}$	$-\bar{R}$	$\bar{R}(R+T)$	O_z

For the crack waveguide modes to be non-leaky, the dispersion relations must be satisfied for real $k_y h$ (or real β_G) since for small angles of incidence $|R \pm T| = 1$, $|\bar{R}| = 1$ is necessary for non-leaky modes to exist. As before, we impose this condition in order to obtain strong resonances. Dispersion curves can be obtained in the manner described in the previous section. If we assume that $\bar{R}(\theta) \approx 1$ (which corresponds to $\partial U_z/\partial y = 0$ at $y = 0$), the curves in Fig. 2 can be used with the following substitutions: $k_x L \to 2k_y h$, $\beta_G L \to 2\beta_G h$. The O_x modes should be ignored. This shows that for the lowest order mode to propagate $\beta_G h \sim 1$ and $h > 0.2\,\lambda_R$, provided that $\bar{R} \cong 1$ is a good approximation for $\theta < \theta_{CR,S}$. We will comment further on the existence of crack waveguide modes when we discuss half-penny shaped cracks.

Resonances of rectangular surface cracks. Following the approach used in References 1 and 2 we treat resonance effects as due to standing wave resonances along the depth or the length of the crack. However, we do not use simply Rayleigh waves, but rather the guided waves of the crack in which the vibrations of the front and back faces are coupled at the edges. We restrict ourselves to non-leaky waveguide modes only, on the grounds that leaky standing waves will not have sufficient high Q's to be strongly excited and to give useful NDE signatures. Our analysis therefore treats only depth standing wave resonances of the trapped slit waveguide modes and length standing wave resonances of trapped crack waveguide modes (Fig. 3).

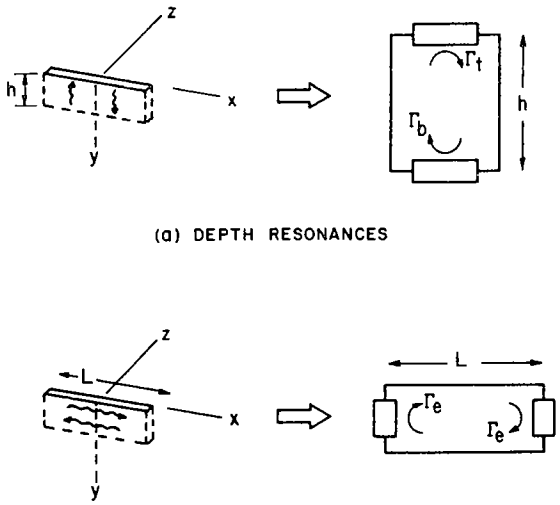

FIG. 3. Waveguide standing wave model for
(a) depth resonances, and
(b) length resonances of the crack.

To continue this approach we must evaluate the modal reflection coefficients at the top and bottom of the crack for the depth resonances and the analogous reflection coefficients at the edges of the crack for the length resonances. With the present model, we are able to introduce more realistic boundary conditions than the rigid boundary conditions assumed previously by others. These boundary conditions are evaluated by considering the behavior of each partial wave in Fig. 1 at an edge boundary normal to the guided wave propagation direction.

For reflection from crack edges and the crack bottom, the results given by Freund apply, and we have the reflection coefficients listed in Table 3 for the various types of modes treated previously. Note that R and T should now be evaluated near 90° since partial waves grazing the guiding edges hit the terminating boundaries normally. There is no coupling at the crack edges between modal families or between modes of the same family. In the case of reflection from a crack top, there is no coupling between the z^+ and z^- faces of the crack, and each partial wave reflects with the reflection coefficient $\bar{R}$, for which the results given by Cuozzo, et al,[7] can be used as an approximation. In this way we obtain the reflection coefficients Γ_t, Γ_b and Γ_e defined in Fig. 3.

Table 3. Reflection coefficients at a crack edge for slit and crack waveguide modes

Mode	Reflection Coefficient
$E_z, E_x E_z, O_x E_z$	(R - T)
$O_z, E_x O_z, O_x O_z$	(R + T)

To investigate the depth resonances, we model the crack as a slit waveguide terminated by a crack edge at one end and a crack top at the other. The resonance condition of the transmission line model as shown in Fig. 3(a) is

$$\Gamma_t \Gamma_b e^{-i2\beta_G h} = 1 \qquad (8)$$

where $\Gamma_t = \rho_t e^{i\alpha_t}$ and $\Gamma_b = \rho_b e^{i\alpha_b}$ are the reflection coefficients for the mode of concern at the top and bottom of the crack respectively, and β_G is the propagation constant for that particular mode. Due to the fact that terminations are lossy, one should allow for a complex resonant frequency, i.e.,

$$\beta_G = \frac{\omega(1 + i/2Q)}{V_G} \qquad (9)$$

The resonant frequency and quality factor are found to be

$$f = \frac{V_G}{2h}\left[\frac{\alpha_t + \alpha_b}{2\pi} + N\right] \qquad (10)$$

and

$$Q = \frac{0.5(\alpha_t + \alpha_b) + N\pi}{-\log_e(\rho_t \rho_b)} \qquad (11)$$

For $\sigma = 0.25$, $\Gamma_t \cong 0.25$, $\Gamma_b(0_z \text{ modes}) = 0.3e^{i(\pi/2)}$ $\Gamma_b(E_z \text{ modes}) = 0.1\, e^{-i(\pi/2)}$. The analysis predicts a quality factor in the order of unity, although experimental quality factors are reported to be somewhat higher than this.

For length resonances, the same kind of procedure gives

$$\Gamma_e^2 e^{-i2\beta_G L} = 1 \qquad (12)$$

writing $\Gamma_e = \rho_e e^{i\alpha_e}$, one obtains the resonance frequency and quality factor as

$$f = \frac{V_G}{2L}\left(M + \frac{\alpha_e}{\pi}\right) \qquad (13)$$

and

$$Q = \frac{\alpha_e + M\pi}{-2\log_e(\rho_e)} \qquad (14)$$

where Γ_e (0_z mode) $= 0.3\, e^{i(\pi/2)}$, Γ_e (E_z mode) $= 0.1\, e^{-i(\pi/2)}$ and $V_G \sim V_R$ for trapped modes.

It is interesting to note that the edge reflection coefficients Γ_e for the 0_z and the E_z modes are π radians out of phase. This indicates that standing wave pattern of an E_z mode and standing wave pattern of the same order 0_z mode have a shift of $\lambda/4$ with respect to each other. In other words, if the E_z mode for a specific resonance frequency is even, the corresponding 0_z mode is odd or vice versa. Keeping in mind that $V_G \sim V_R$ for both modes we see that, at each resonance frequency predicted by Eq. (13), there is always an even and an odd standing wave pattern that can be supported by the crack structure. In experimental observations of crack resonances excited by normally incident Rayleigh waves, length resonances of all orders have been noted. This poses a difficulty for the single surface model used previously. In this model the resonances are alternately x-symmetric and x-antisymmetric, while the excitation of normal incidence is x-symmetric only. One therefore predicts excitation of alternate modes only. We see that the two surface model used here resolves the dilemma since it predicts an x-symmetric vibration for every order of resonance, alternating from an E_z type mode to an 0_z type mode as the order increases.

(b) Half-penny shaped crack: Here, the solutions of Eq. (2) are $H_\nu^{\mp}(k_R r)\, e^{\pm i\nu\phi}$, where r and ϕ are polar coordinate variables and $H_\nu^{\mp}(k_R r)$ are Hankel functions of the first and second kind of order ν. We do not restrict ourselves to integer values of ν since the structure is not periodic in ϕ $(-\pi/2 \leq \phi \leq \pi/2)$. It is appropriate in this problem to express the Hankel functions in the following form:

$$H_\nu^{\mp}(x) = M_\nu(x)\, e^{\mp i\psi_\nu(x)} \qquad (15)$$

where $M_\nu(x)$ is the magnitude and $\psi_\nu(x)$ is the phase of the Hankel functions, i.e.,

$$M_\nu(x) = \left[J_\nu^2(x) + Y_\nu^2(x)\right] \qquad (16)$$

and

$$\psi_\nu(x) = \tan^{-1}\frac{Y_\nu(x)}{J_\nu(x)} \qquad (17)$$

In our notation, the - and + signs in Eq. (15) correspond to radially outgoing and incoming waves, respectively.

To get a feeling about the behavior of these circular partial waves, let us examine them more closely. Any of the partial waves shown in Fig. 4 can be expressed in the form

$$P_i = M_\nu(k_R r)\exp\left[\pm i(\psi_\nu(k_R r) \pm \nu\phi)\right] \qquad (18)$$

The propagation vector at any point (r,ϕ) can then be found by taking the negative gradient of the phase function:

$$\vec{k} = -\nabla\left[\pm\psi_\nu(kr) \pm \nu\phi\right] = \mp k_R \frac{d\psi_\nu(k_R r)}{\partial(k_R r)}\hat{r} \mp \frac{\nu}{r}\hat{\phi} \qquad (19)$$

where $\hat{r}$ and $\hat{\phi}$ are unit vectors in polar coordinates. If we make an analogy between the circular and rectangular cases, $k_R\psi_\nu'$ corresponds to k_y and ν/r corresponds to k_x. Therefore one can form the analogous cases of slit and crack waveguides, as shown in Fig. 4. It is seen that the analogous case of slit waveguide is such that the modes are guided by the crack top — that is, the waves are radial. For the case of crack waveguide, the guidance is assumed via the crack edge and the waves are angular. In both cases, the partial waves should graze the guiding boundaries for nonleaky propagation. We will assume that Freund's

results are also applicable for the curved crack boundaries.

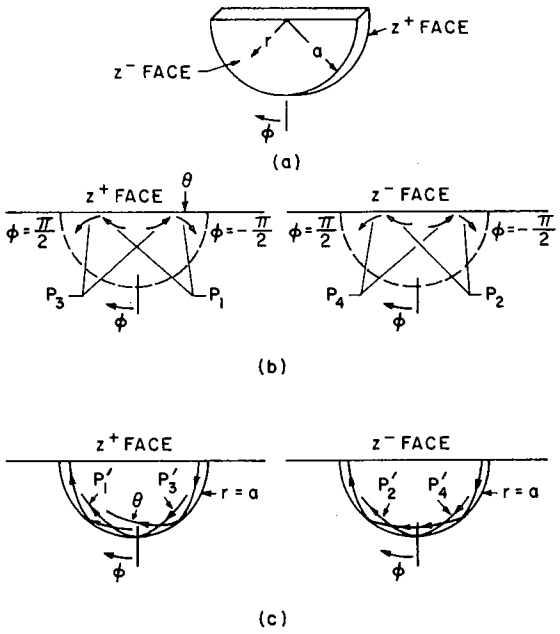

FIG. 4. (a) Half-penny shaped crack geometry;
(b) Partial waves for radial waveguide modes (cf Fig. 1(b));
(c) Partial waves for angular waveguide modes (cf Fig. 1(c)).

The radial waveguide modes can now be investigated. The partial waves are:

$$P_{1,2} = A_{1,2} M_\nu(k_R r) e^{-i\psi_\nu(k_R r)} e^{-i\nu\phi}$$
$$P_{3,4} = A_{3,4} M\nu(k_R r) e^{-i\psi_\nu(k_R r)} e^{+i\nu\phi} . \quad (20)$$

Writing the boundary conditions at $\phi = \pm \pi/2$, one obtains

$$e^{i\nu\pi} \begin{pmatrix} A_1 \\ A_2 \\ A_3 \\ A_4 \end{pmatrix} = \begin{pmatrix} 0 & 0 & \bar{R} & 0 \\ 0 & 0 & 0 & \bar{R} \\ \bar{R} & 0 & 0 & 0 \\ 0 & \bar{R} & 0 & 0 \end{pmatrix} \begin{pmatrix} A_1 \\ A_2 \\ A_3 \\ A_4 \end{pmatrix} \quad (21)$$

for which the solutions can be obtained as

A_1	A_2	A_3	A_4	$e^{i\nu\pi}$	Mode Identification
1	1	1	1	$\bar{R}$	$E_\phi E_z$
1	-1	1	-1	$\bar{R}$	$E_\phi O_z$
1	1	-1	-1	$-\bar{R}$	$O_\phi E_z$
1	-1	-1	1	$-\bar{R}$	$O_\phi O_z$

If we again assume a boundary condition of $(\partial U_z/\partial n) = 0$ at $\phi = \pm \pi/2$, (i.e., $\bar{R} = 1$), we obtain the restriction

$$\nu = \begin{cases} 0,2,4,\ldots & \text{for } E_\phi \text{ modes} \\ 1,3,5,\ldots & \text{for } O_\phi \text{ modes} \end{cases} \quad (22)$$

The resonance condition for the modes can be written in a similar manner, and one obtains

$$e^{i2\psi_\nu(k_R a)} = \begin{cases} (R-T) \cong 0.1 e^{-i(\frac{\pi}{2})} & \text{for } E_z \text{ modes} \\ (R+T) \cong 0.3 e^{i(\frac{\pi}{2})} & \text{for } O_z \text{ modes} \end{cases} \quad (23)$$

Again equating the phases, one can graphically obtain the depth resonances as shown in Fig. 5. The resonances corresponding to $\nu > 0$ must be eliminated since "the incidence angles of partial waves", $\theta \simeq \tan^{-1}(\nu/kr)$ do not allow "grazing incidence" at $\phi = \pm(\pi/2)$, especially around $r = 0$. For $\nu = 0$, we approximate the angle of the Hankel function by its asymptotic expansion,

$$\psi_0(k_R a) \approx k_R a - \frac{\pi}{4} \quad (24)$$

The accuracy of the approximation can be seen from Fig. 5. We then obtain the resonance frequency and quality factor

$$f = \frac{V_R}{2a} \cdot N \quad (25)$$

$$Q = \frac{N\pi}{-\log_e(\rho'_e)} \quad (26)$$

where (ρ'_e) is the magnitude of $(R \pm T)$ given in Eq. (23).

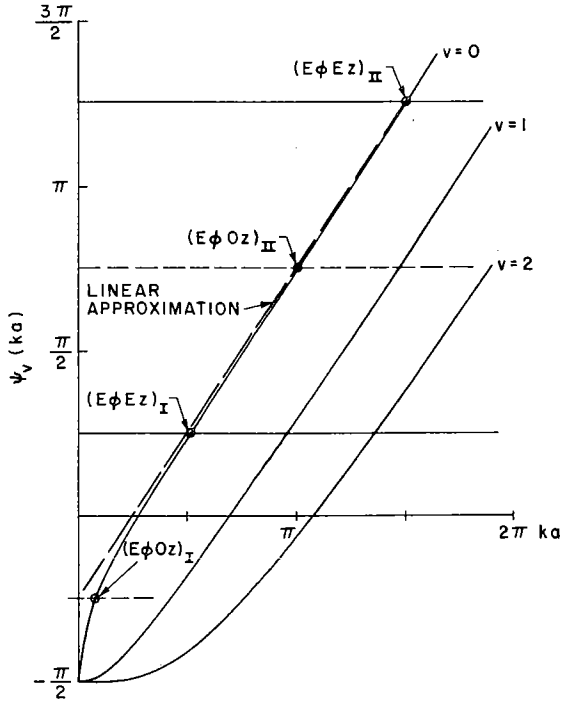

FIG. 5. Graphical evaluation of radial (i.e. depth) resonance frequencies for a half circular crack.

Comparing Eqs. (25) and (26) with Eqs. (10) and (11) we see that depth resonance frequencies are almost the same, and that the circular crack yields a higher quality factor.

For length resonances, the same kind of analysis yields the following equation

$$e^{i2\psi_\nu(k_R a)} = \begin{cases} (R - T) & E_z \text{ mode} \\ (R + T) & O_z \text{ mode} \end{cases} \qquad (27)$$

provided that the incidence angle of partial waves at $r = a$ is small. That angle can be expressed as

$$\theta = \tan^{-1}\left[k_R r \frac{d\psi_\nu(k_R r)/d(k_R r)}{\nu}\right]_{r=a} \qquad (28)$$

Taking ν as a parameter and eliminating $k_R a$, one can plot $\psi_\nu(ka)$ vs θ. From Freund's boundary conditions $\frac{1}{2}\arg(R \pm T)$ vs θ can also be plotted. As in the rectangular crack case, the intersection of two curves should give the guide parameters. We have plotted these curves in Fig. 6 and one readily observes that there is no solution for the "angular waveguide" modes. In other words, the guide proposed in Fig. 4(c) does not act as a nonleaky waveguide.

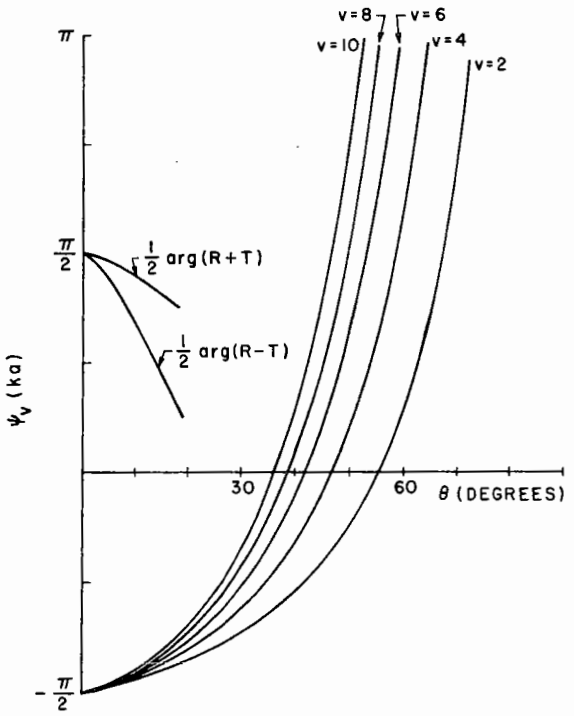

FIG. 6. Graphical solution of dispersion equation of angular waveguide modes.

Experimentally, length resonances have been found to not depend significantly on the shape of the crack, and they are found to exist even in circular cracks. The basic analytical difference between rectangular and circular cracks is that in the rectangular case, guidance is achieved via the bottom of the crack. The "mode switching" between E_z and O_z modes noted in the previous section as the explanation for observations of resonances in all orders is caused by edge coupling between the front and back faces of the crack. However in the circular crack, the analysis shows that there are no corresponding non-leaky resonances in the angular direction. Furthermore scattering at the top of the crack does not introduce the coupling between the back and front faces required for "mode switching". An explanation of the length resonance behavior observed in circular cracks must therefore be sought elsewhere.

One possible explanation for length resonances could be through the concept of edge waves introduced by Bondarenko and Dubovitskii,[8] Wagers,[9] and Sharon.[10] These waves can propagate along the top edge of the crack, decaying in two other directions. Using the concepts introduced by crack waveguide two such waves, one on each top edge, can be postulated. As in the crack waveguide, these waves are coupled at the crack corners and the reflection coefficients at the corners must behave differently for even and odd field distributions relative to the z direction, resulting in a similar "mode switching" to that noted above. The drawback of this hypothesis is that the edge waves travel slower than Rayleigh waves (for $\sigma = 0.25$, $V_{edge} \sim 0.87\, V_R$), which results in lower resonance frequencies. Assuming that boundary conditions are the same as those of the crack waveguide, the length resonances with edge waves can be found to occur at

$$f = \frac{V_{edge}}{2L}\left(M + \frac{1}{2}\right) \qquad (29)$$

COMPARISON WITH EXPERIMENTAL DATA

We have compared our analytical results with the data given in References 2 and 11. Our results (Tables 4 and 5) agree fairly well with the length resonances of Reference 2, and good agreement is obtained for both resonances of Reference 11. For each resonances, we can assign the mode indices M and N (see Eqs. 10, 13, 25, 29) with reasonable accuracy. The formulas used in calculations are repeated below.

$$\text{Length resonances:} \quad f_L = \frac{V_R}{2L}\left(M + \frac{1}{2}\right) \qquad (30)$$

$$\text{Depth resonances:} \quad f_D = \frac{V_R}{2h} N \qquad (31)$$

TABLE 4. Comparison of Theoretical Calculations with the Data of Reference 2

Crack #	f_L (MHz) (Experimental)	f_L Eq. (30)	M	f_D (MHz) (Experimental)	f_D Eq. (31)	N
1	3.48	3.55	5	5.8	6.62	1
	4.02	4.20	6			
	4.58	4.84	7			
	5.20	5.49	8			
2	3.60	3.62	2	5.68	5.94	1
	5.18	5.08	3			
3	3.86	3.56	1	5.6	5.94	1
	*	5.94	2			
4	3.18	3.43	1	5.1	4.58	1
	5.72	5.72	2			
5	3.00	3.43	1	4.0	3.3	1
	5.80	5.72	2			
6	3.00	3.43	1	3.6	2.57	1
	5.80	5.72	2			

The cracks tested were EDM notches on a steel sample, with their aspect ratios varying between 0.097 and 0.89. The asterisk for the second resonance of the third crack means that the resonance also corresponds to a depth resonance.

TABLE 5. Comparison of Theoretical Calculations with the Date of Reference 11

f_L (MHz) (Experimental)	f_L Eq. (30)	M	f_D (MHz) (Experimental)	f_D Eq. (31)	N
0.83	0.84	1	3.41	3.74	1
1.24	1.40	2	7.93	7.47	2
1.79	1.96	3			
2.27	2.52	4			
2.90	3.07	5			
*	3.63	6			
4.00	4.20	7			
4.48	4.75	8			
5.24	5.31	9			
6.13	5.87	10			
6.41	6.43	11			
7.03	6.99	12			

The crack is a (2.54 mm × 0.38 mm) EDM notch on the aluminum sample.

In the length resonance calculations above, we used Rayleigh wave velocities instead of edge wave velocities. A complete analysis of the edge waves can be found in Reference 12, where the equations of motion are solved by expanding each displacement component in a double series of Laguerre functions. The analysis shows that there are two symmetry modes that can be supported by the edge, and for $\sigma = 0.25$ the corresponding edge wave velocities are $V_{edge}/V_R \sim 0.98$ and 1.002, which are very close to the Rayleigh wave velocity.

There have been other approaches for the solution of edge wave modes and velocities.[8,9] In Reference 8 the solutions are approximated such that the boundary conditions are not fully satisfied on the two free surfaces of the edge. For $\sigma = 0.25$, this approach yields a numerical value of $V_{edge}/V_R = 0.86$. In Reference 9 a variational approach is utilized and their result gives $V_{edge}/V_R \sim 0.7$ for $\sigma = 0.34$. This result is in agreement with what can be obtained from Reference 8. One reason for this agreement is that the trial functions used in the variational approach are of the same nature as the functions resulting from the analysis of Reference 8.

In conclusion, considering the results given by Maradudin, et al.,[12] the use of Rayleigh wave velocities instead of edge wave velocities does not ignore the role of edge waves for length resonances. The open question is the verification of the hypothesis of π radians phase shift between the even symmetric and odd symmetric edge wave modes in the z direction.

ACKNOWLEDGEMENT

This research has been sponsored by the Center for Advanced NDE operated by the Science Center, Rockwell International for the Advanced Research Projects Agency and the Air Force Materials Laboratory under Contract No. F33615-74-C-5180.

REFERENCES

1. B. R. Tittmann, M. de Billy, F. Cohen-Tenoudji, A. Jungman, and G. Quentin, "Measurements of Angular and Frequency Dependence of Acoustic Surface Wave Scattering from Surface Cracks," IEEE Ultrasonics Symposium Proceedings, 78CH 1344-1SU, pp. 379-383 (1978).

2. V. Domarkas, B. T. Khuri-Yakub, and G. S. Kino, "Length and Depth Resonance of Surface Cracks and Their Use for Crack Size Estimation," Appl. Phys. Lett. 33, 7, 557-559 (October 1978).

3. B. A. Auld, S. Ayter, and M. Tan, "Theory of Scattering of Rayleigh Waves by Surface Breaking Cracks," IEEE Ultrasonics Symposium Proceedings, 78CH 1233-1 SU, pp. 384-390 (1978).

4. L. B. Freund, "The Oblique Reflection of a Rayleigh Wave from a Crack Tip," International Journal of Solids and Structures 7, 1199-1210 (1971).

5. L. B. Freund, "Surface Waves Guided by a Slit in an Elastic Solid," J. Appl. Mechanics, 1027-1032 (December 1972).

6. J. K. Knowles, "A Note on Elastic Surface Waves," J. Geophysical Research, 71, 22, 5480-5481 (November 1966).

7. F. C. Cuozzo, E. L. Cambiaggio, J-P Damiano, and E. Rivier, "Influence of Elastic Properties on Rayleigh Wave Scattering by Normal Discontinuities," IEEE Trans. Sonics Ultrason. SU-24, 4, 280-289 (July 1977).

8. V. S. Bondarenko and V. F. Dubovitskii, "Acoustic Edge Waves in Isotropic Solids," Sov. Phys. Acoust. 22, 2, 159-160 (March-April 1976).

9. R. S. Wagers, "Variational Analysis of Acoustic Waveguides," IEEE Ultrasonics Symposium Proceedings, 121-125 (1973).

10. T. M. Sharon, "Edge Modes for Piezoelectric Wedges of Arbitrary Interior Angles," IEEE Ultrasonics Symposium Proceedings, 126-130 (1973).

11. B. R. Tittmann, private communication.

12. A. A. Maradudin, R. F. Wallis, D. L. Mills, and R. L. Ballard, "Vibrational Edge Modes in Finite Crystals," Phys. Rev. B. 6, 4, 1106-1111 (August 1972).

SUMMARY DISCUSSION
(S. Ayter and B. Auld)

Ed Kraut (Session Chairman--Science Center): Questions on this talk?

Unidentified Speaker: Let me see if I get this straight. Talking about the rectangular crack, you excite the Rayleigh wave along the ZED plus or minus face, and the waves travel down in the Y direction and up again on the other side and back again, or is this --

S. Ayter: You don't excite simple Rayleigh waves. You excite the wave guide modes which are combinations of Rayleigh waves, and those waves go down and come up, but they go down on both faces and come up on both faces.

Unidentified Speaker: How do you excite the wave? What is the excitation scheme?

S. Ayter: We have calculated the coupling quotient, but we don't have the results here. The way to excite is you have a crack here, and you illuminate it normally with the Rayleigh wave, and these Rayleigh waves excite the waveguide modes going down.

Unidentified Speaker: There is no wave going down there. It's only on the two surfaces, and the two surfaces are separated by distance between ZED plus and ZED minus. How does it go from one side to the other? It has to go down one crack and up the other side.

S. Ayter: On each face, each face is a traction-free surface. So, each face separately can support Rayleigh waves. And, a combination of those Rayleigh waves can guide waves that are going down.

B. Auld: Could I make a comment, in response here? The fact is, the two faces are coupled at the edges. These Rayleigh waves that are propagating on the faces at an angle are coupled at the edges all the way down, and it's that edge coupling that gives rise to the guided waves which exist on both surfaces.

# #